1 **Spike-specific IgG4 generated post BNT162b2 mRNA vaccination is inhibitory when directly**

2 **competing with functional IgG subclasses**

3

4 Jerry C. H. Tam[1], Abbie C. Sibayan[1], Jeffrey Seow[1], Carl Graham[1], Ashwini Kurshan[1], Blair Merrick[2],

5 Richard J. Stanton[3], Katie J. Doores[1]#

6 [1] Department of Infectious Diseases, School of Immunology & Microbial Sciences, King's College

7 London, London, UK.

8 [2] Centre for Clinical Infection and Diagnostics Research, Department of Infectious Diseases, Guy's and

9 St Thomas' NHS Foundation Trust, London, UK.

10 [3] Division of Infection and Immunity, School of Medicine, Cardiff University, Cardiff, United Kingdom.

11

12 # Corresponding author: katie.doores@kcl.ac.uk

13

14

1

Abstract:

The rapid development of vaccines against SARS-CoV-2 during the COVID-19 pandemic proved vital in controlling viral spread and reducing mortality and morbidity. Both neutralising activity and effector function activity of Spike-specific antibodies have been shown to be important for their protective and therapeutic activity. However, several recent studies have reported that vaccination with mRNA based COVID-19 vaccines can lead to elevated levels of Spike-specific IgG4, an isotype which is often considered anti-inflammatory due to its reduced binding to Fcγ receptors on immune cells. Here we show that the level of Spike-specific IgG4 produced following BNT162b2 vaccination is impacted by the interval between and frequency of vaccines boosts, prior SARS-CoV-2 infection (hybrid immunity), breakthrough infection and bivalent vaccine boosters. Despite the increase in Spike-specific IgG4 between the 2nd and 3rd BNT162b2 vaccine dose, neutralisation, ADCD and ADCP activity all increased. Through expression of SARS-CoV-2 monoclonal antibodies cloned as IgG1, IgG2, IgG3 and IgG4, we demonstrated that whilst Spike-specific IgG4 had reduced effector function activity, including ADCC, ADCD and ADCP, IgG4 was only inhibitory when directly competing with functional IgG subclasses binding to an overlapping epitope. In the context of polyclonal plasma, ADCC and ADCD activity could not be depleted by addition of high concentrations of a Spike-specific IgG4 mAb cocktail suggesting the non-stimulatory effect of Spike-specific IgG4 may be hidden in more complex scenarios, such as polyclonal mixes in serum.

Introduction

The COVID-19 pandemic led to the rapid development and deployment of several COVID-19 vaccines utilising a range of different vaccine platforms (Bok et al., 2021). Vaccines targeting SARS-CoV-2 Wuhan Spike glycoprotein have been highly effective in reducing morbidity and mortality from COVID-19 (Higdon et al., 2022). In particular, the pandemic led to the first widespread clinical use of mRNA based vaccines; including BNT162b2 from BioNTech/Pfizer (Polack et al., 2020) and Spikevax from Moderna (Baden et al., 2021). These were initially deployed in a 2-dose regimen, separated by a 3-week interval (Baden et al., 2021; Polack et al., 2020). However, the United Kingdom quickly changed to a 12-week interval between doses, with the rationale of ensuring some degree of SARS-CoV-2 immunity for a wider proportion of the population (UKHSA, 2022). To overcome waning antibody levels (Seow et al., 2020), a third dose was offered as a booster, which had the additional benefit of broadening the antibody response towards SARS-CoV-2 variants of concern (Graham et al., 2022; Kim et al., 2022; Roltgen et al., 2022; Sokal et al., 2021), as well as leading to an increased antibody binding avidity (Graham et al., 2022). More recently, updated mRNA vaccines based upon newer variants such as BA.1 and XBB.1.5 have been used as boosters (Kirsebom et al., 2023), not only for individuals primed with COVID-19 Wuhan-1 mRNA vaccines (Kirsebom et al., 2023; Lee et al., 2023), but also for individuals who had initially received other vaccines types, such as the AstraZeneca Chimpanzee Adenovirus Vector (ChAdOx) COVID-19 vaccine, AZD1222 (Akhtar et al., 2023). Given the safety and efficacy of COVID-19 mRNA vaccines, there has been increased interest in using this vaccine platform for more applications, including vaccines against other pathogenic viruses as well as against bacteria, and as immunotherapies for cancer treatment (Parhiz et al., 2024).

Whilst antibody binding and neutralisation correlate with protection against SARS-CoV-2 infection and severe COVID-19 disease (Goldblatt et al., 2022), the Fc region can also collaborate to enhance the protective capacity of antibodies. Animal studies have shown the importance of Fc-mediated effector functions of monoclonal antibodies (mAbs) for limiting SARS-CoV-2 immunopathology and viral persistence in animal models (Chan et al., 2021; Pierre et al., 2024; Schafer et al., 2021; Yamin et al., 2021), as well as robust antibody Fc-effector functions induced by vaccines

3

61 correlating with protection in animal challenge studies (Gorman et al., 2021; Mercado et al., 2020;

62 Tostanoski et al., 2020).

63   It has previously been reported that the use of COVID-19 mRNA-based vaccines can lead to

64 skewing of the IgG subclass usage against SARS-CoV-2 Spike (Akhtar et al., 2023; Buhre et al., 2022;

65 Gelderloos et al., 2024; Irrgang et al., 2023). In addition to the majority IgG1 and IgG3 response, Spike-

66 specific IgG4 could also be detected at low levels in some individuals around 6-7 months post a second

67 dose of either BNT162b2 or Spikevax (Akhtar et al., 2023; Irrgang et al., 2023) and at higher levels in

68 the majority of individuals following a third dose of BNT162b2, as well as following a BNT162b2

69 booster vaccine in individuals who initially received the AZD1222 vaccine (Akhtar et al., 2023). This

70 increase in Spike-specific IgG4 is notable, given that IgG4 is usually thought to be anti-inflammatory

71 (Pillai, 2023), and is not typically observed following vaccination or infection (Urban et al., 1994).

72 Instead, antigen-specific IgG4 has been reported in the context of allergy (Qin et al., 2022),

73 autoimmunity (Motta and Culver, 2024; Rispens and Huijbers, 2023) and chronic inflammatory

74 conditions (van de Veen et al., 2020). The perceived role of IgG4 as anti-inflammatory comes from its

75 reduced ability to stimulate Fc-mediated antibody effector functions (Bruhns et al., 2009; Pillai, 2023),

76 including antibody-dependent cellular cytotoxicity (ADCC), antibody-dependent complement

77 deposition (ADCD) and antibody-dependent cellular phagocytosis (ADCP), due to the reduced affinity

78 of the IgG4 Fc domain for FcγR receptors, in particular FcγRIIA, FcγRIIIA and FcγRIIIB (Vidarsson

79 et al., 2014). IgG4 is the only immunoglobulin that can undergo Fab-arm exchange, a process in which

80 half-molecules of IgG4 combine randomly resulting in bispecific immunoglobulins with reduced

81 binding and/or neutralising activity due to a lower valency of binding (van der Neut Kolfschoten et al.,

82 2007).

83   Antibody effector functions are important in clearing infection through binding of antibodies

84 to antigens expressed on the surface of infected cells or to free virus (Beaudoin-Bussieres and Finzi,

85 2024). Effector functions have been shown to be important in both prophylactic and therapeutic

86 protection models (Gorman et al., 2021; Zhang et al., 2023). For example, introduction of the LALA-

87 PG mutations (L234A+L235A+P329G), which are known to reduce the binding of IgGs to FcγRs,

88   reduces the therapeutic activity of neutralising antibodies against SARS-CoV-2 (Winkler et al., 2021).

89   Furthermore, non-neutralising Spike-specific IgG1 can confer protection in small animal challenge

90   models if passively administered prior to challenge (Clark et al., 2024). Whilst the relevance of IgG

91   subclass has not been studied *in vivo* in the context of SARS-CoV-2 infection in humans, antibody

92   passive transfer experiments in the context of Influenza virus infection have revealed that IgG subclass

93   is important in determining protection (DiLillo et al., 2014; Van den Hoecke et al., 2017). However,

94   animal studies have limited utility for understanding the impact of increased levels of antigen-specific

95   IgG4 given that it is only found in humans and great apes (Olivieri and Gambon Deza, 2018).

96   Whilst several studies report elevated levels of Spike-specific IgG4 following mRNA

97   vaccination (Akhtar et al., 2023; Buhre et al., 2022; Gelderloos et al., 2024; Irrgang et al., 2023), there

98   is an incomplete knowledge of factors that might influence the switch to IgG4 and how the level of

99   Spike-specific IgG4 might be impacted by further mRNA vaccine booster doses and/or breakthrough

100   infection (BTI). Furthermore, there is an incomplete understanding of the functional implications of the

101   presence of Spike-specific IgG4 on the functional activity of the Spike-specific Total IgG. Here, we

102   investigated the impact of; i) mRNA vaccine interval and frequency, ii) hybrid immunity, iii)

103   breakthrough infection and iv) bivalent vaccines on the amount of IgG4 produced, the IgG4 binding

104   specificity, breadth and avidity, and effector function activity in immune plasma. We observed that IgG4

105   production was impacted by the number of mRNA doses, the interval between these doses and SARS-

106   CoV-2 infection (both pre- and post- vaccination). Through generation of a panel of class-switched

107   Spike-specific mAbs, including IgG1, IgG2, IgG3 and IgG4, we demonstrate that whilst IgG4 poorly

108   activates ADCC, ADCP and ADCD, it is capable of potent and equivalent neutralisation as IgG1.

109   Importantly, IgG4 is only anti-inflammatory when competing directly for binding with an activating

110   IgG1 but is functionally silent if non-competing. These findings provide important insights into the

111   functional implications of elevated levels of Spike-specific IgG4 following BNT162b2 mRNA

112   vaccination.

113

114   **Results**

Spike-specific IgG4 class-switching increases with multiple BNT162b2 vaccine exposures and time

To gain further understanding of the factors influencing class-switching to Spike-specific IgG4 during mRNA vaccination, we studied selected plasma from several UK based vaccine cohorts (**Table S1A** and **Fig. S1A**). These groups differed in; i) the spacing between the first and second vaccine doses, ii) prior or subsequent SARS-CoV-2 infection, and iii) use of a bivalent booster vaccine based on Wuhan-1/BA.1. We first measured the concentration of SARS-CoV-2 Spike-specific IgG in a subclass specific manner for each group using a semiquantitative ELISA (**Fig. 1**).

Following the standard BNT162b2 vaccination protocol (i.e. a 3–4-week interval between first and second dose, referred here to as "short group"), total IgG levels averaged 45.1 µg/ml after two mRNA doses (**Fig. 1A**). As previously reported, the total Spike-specific IgG levels waned over time, such that at six months post vaccination, they decreased to 9.05 µg/ml. A third vaccine dose was able to increase the level back to 67.0 µg/mL. This pattern of IgG levels can largely be explained by changes in IgG1, IgG2 and IgG3, which all follow a similar pattern. However, Spike-specific IgG4 only became detectable after the third dose of vaccine, similar to that previously reported (Gelderloos et al., 2024; Irrgang et al., 2023) with levels reaching 1.47 µg/ml.

In the UK, the majority of individuals receiving the BNT162b2 vaccine did so with an extended 8–12-week interval between the first and second doses (referred to here as "extended group"). The trends in total IgG, IgG1, IgG2 and IgG3 levels were similar to that of the short group (**Fig. 1B**). However, in contrast to the short group, Spike-specific IgG4 could be observed earlier, with Spike-specific IgG4 being detected in all individuals at 6 months post 2nd dose and prior to the third vaccination suggesting the vaccine interval can influence class-switching to IgG4. Interestingly, unlike at 6-months post the 2nd vaccine dose, where IgG1 responses had waned, IgG4 responses had increased. However, at 6-months post the 3rd vaccine dose, all antibody isotypes had waned, including IgG4 (**Fig. 1C**).

140   Next, we examined the impact of hybrid immunity on IgG4 production, including infection

141   prior to vaccination as well as a BTI post vaccination. A more heterogenous response was observed in

142   individuals who had a SARS-CoV-2 infection prior to vaccination, with 3/8 of the volunteers producing

143   Spike-specific IgG4 after the first vaccine dose, and all producing Spike-specific IgG4 after two doses

144   (**Fig. 1D**). A breakthrough infection after three BNT162b2 vaccinations lead to a further increase in

145   Spike-specific IgG4, reaching levels of only ~5-fold below Spike-specific IgG1 in some individuals

146   (**Fig. 1E**). Some individuals were subsequently vaccinated a fourth time with a bivalent WT/BA.1

147   mRNA vaccine, and this additional vaccination led to a further increase in Spike-specific IgG4 levels

148   as well as total IgG, IgG1, IgG2 and IgG3 levels (**Fig. 1F**).

149   Together, these data demonstrate that Spike-specific IgG4 generated in response to mRNA

150   vaccination is impacted by the interval and number of vaccinations, the time since vaccination, and an

151   infection prior to/or after BNT162b2 vaccination.

152

153   **Spike-specific IgG4 is not detected in a longitudinal infection cohort**

154   Several studies have reported a continued evolution of the antibody response post SARS-CoV-

155   2 infection as demonstrated by increased somatic hypermutation of Spike-specific mAbs isolated 6-

156   months post infection (Gaebler et al., 2021). To determine whether time from infection might influence

157   the production of Spike- and/or nucleocapsid-specific IgG4 post infection we measured total IgG and

158   IgG4 levels in a longitudinal infection cohort from Wave 1 (i.e. beginning March 2020) that was

159   followed until 33 weeks post infection (**Table S1B** and **Fig. S1B**). Spike-specific IgG4 could not be

160   detected in plasma from individuals experiencing mild (**Fig. 2A**) or severe (**Fig. 2B**) disease, even up

161   to similar times post-infection as for the post-vaccination volunteers. These data suggest that the

162   production of Spike-specific IgG4 is not an inherent feature to the Spike protein itself or the time post

163   SARS-CoV-2 Spike exposure and that multiple exposures is important.

164

165   **IgG4 class-switch is Spike-specific**

166   As the levels of Spike-specific IgG4 were boosted upon breakthrough infection, we next

167   determined whether IgG4 production was restricted to Spike or if IgG4 to nucleocapsid (which is not

168   present in the BNT162b2 vaccine) could be detected following breakthrough infection. After two

169   breakthrough infections post-vaccination, there was a robust Spike-specific IgG4 response, which

170   persisted for at least 6 months after the second infection (**Fig. 2C**). However, there was no nucleocapsid-

171   specific IgG4 detected, even 6 months after a second breakthrough infection.

172   Some individuals also received an Influenza vaccine at the same time as their third BNT162b2

173   vaccination. We therefore investigated whether the immune environment generated in response to the

174   mRNA vaccination might impact on IgG4 class-switching to influenza HA. No haemagglutinin-specific

175   IgG4 were detected in any of these plasma samples (**Fig. 2D**). Combined, these data indicate that the

176   class-switching to IgG4 is specific for SARS-CoV-2 Spike in the context of mRNA vaccination.

177

178   **Spike-specific IgG4 is distributed across RBD and NTD domains**

179   We next investigated the domains on SARS-CoV-2 Spike targeted by the IgG4 response with a

180   focus on the extended group. The two major Spike domains targeted by neutralising antibodies are the

181   Receptor Binding Domain (RBD), which interacts with the host cell receptor Angiotensin Converting

182   Enzyme 2 (ACE2) (Walls et al., 2020), and the N-Terminal Domain (NTD), which it's function is less

183   well defined (Jackson et al., 2022). Binding of IgG4 to both RBD and NTD could be detected by ELISA

184   (**Fig. 2E**). When considering the proportion of IgG4 binding to each domain, 33.6% of the Spike-

185   specific IgG4 were targeted against RBD, similar to 30.2% (SD 4.53) of the Total IgG; and 19.7% (SD

186   9.87) of the Spike-specific IgG4 was targeted against NTD, similar to 23.8% of the Total IgG (**Fig. 2F**)

187   suggesting the Spike-specific IgG4 response is not skewed towards a specific Spike domain.

188

189   **Spike-specific IgG4 has similar variant binding breadth to total Spike-specific IgG**

190   Previous studies have shown that repeated COVID-19 vaccination can lead to increased

191   antibody binding and neutralisation breadth against newer SARS-CoV-2 variants of concern (Graham

192   et al., 2022; Muecksch et al., 2022; Wratil et al., 2022). Given that Spike-specific IgG4 also emerges

193   and increases following multiple mRNA vaccinations, we therefore measured breadth of the Spike-

194   specific IgG1 and IgG4 responses by measuring variant Spike-binding breadth by ELISA. We focused

195   on the Spike-specific Total IgG and IgG4 in the extended group following three BNT162b2 doses (**Fig.**

196   **2G**). Similar to the Total IgG binding, comparable levels of IgG4 binding were observed against the

197   WT, Beta, Delta and BA.1 SARS-CoV-2 recombinant Spikes.

198

Spike-specific IgG4 has a delayed avidity increase

200   Antibody avidity can also be enhanced by repeated antigen exposure, either through

201   vaccination or infection (Graham et al., 2022; Wratil et al., 2022). Previous studies have associated the

202   increased Spike-specific Total-IgG avidity with increasing levels of IgG4 (Irrgang et al., 2023).

203   However, this study did not specifically measure avidity changes for Spike-specific IgG1 and IgG4

204   independently. Here, we first measured the avidity index against WT Spike of the Total IgG by

205   comparing the area under the curve in ELISA, with and without an 8M Urea washing step (Graham et

206   al., 2022). Similar to previously published results (Graham et al., 2022), the avidity of Spike-specific

207   Total IgG increased with additional vaccine doses, as well as time post vaccination, up until the third

208   dose where the avidity score reached a plateau (**Fig. 2H**). When considering the avidity of Spike-

209   specific IgG1 and IgG4 independently, the IgG1 avidity mirrored the increasing avidity pattern

210   observed for the Total IgG (**Fig. 2I**). In contrast, the avidity of Spike-specific IgG4 when first detected

211   at 6-months post 2nd vaccine was low (35.0%, SD 7.62) compared to the Total IgG (73.4%, SD 5.62)

212   and to IgG1 (72.2%, SD 6.32) (**Fig. 2I**). However, the IgG4 avidity increased following a third

213   BNT162b2 (65.3%, SD 5.84) with a smaller increase following a subsequent bivalent booster (86.4%,

214   SD 3.44) to reach similar avidity levels to the Spike-specific IgG1 (83.4%, SD 6.23). Although the

215   avidity against WT Spike became equal after a bivalent booster, the avidity against the BA.1 Spike

216   remained lower for IgG4 (62.0%, SD 9.96) compared to IgG1 (81.4%, SD 8.13) (**Fig. 2J**) suggesting

217   that affinity maturation of IgG4 against the BA.1 Spike is less. Overall, the avidity of Spike-specific

218   IgG4 was delayed compared to IgG1 but plateaued at a similar level after three vaccine doses against

219   the matched vaccine antigen.

220

221   **Serum antibody functional activity is associated with IgG1 levels, but not IgG4**

222   We next investigated the functional effect of the increase in Spike-specific IgG4 on functional

223   activity of polyclonal sera, including neutralisation, ADCC, ADCP and complement deposition. Given

224   the largest increase in Spike-specific IgG4 was observed between the second and third dose of

225   BNT162b2, we investigated the differences in functional activity between plasma from these time

226   points in the extended group. Neutralisation activity is largely antibody Fc binding independent

227   (Mozdzanowska et al., 2003), and as previously shown, there was a trend towards increasing plasma

228   neutralising activity between the 2nd and 3rd dose of mRNA vaccine against WT (although this did not

229   reach significance) consistent with the increase in Spike-specific Total IgG (**Fig. 3A**) (Graham et al.,

230   2022). Both the IgG1 and IgG4 levels correlated with the ID_{50} values (**Fig. 3B**).

231   ADCC is dependent on CD16 expressed on NK cells, so we tested the ability of these plasma

232   to stimulate an NK-92 cell line expressing CD16 to degranulate using CD107a expression as the readout

233   (Bartsch et al., 2023). In our assay, there was no significant difference in NK cell degranulation between

234   the 2nd and 3rd dose of mRNA vaccine at the highest dilution tested (1:50) (**Fig. 3D**), although there was

235   notable heterogeneity between whether ADCC increased or decreased presumably due to the differing

236   IgG1 and IgG4 levels. We therefore correlated the level of NK cell degranulation with concentration of

237   Spike-specific IgG1 and IgG4. NK cell degranulation positively correlated with Spike-specific IgG1

238   levels, but no correlation was observed with Spike-specific IgG4 levels (**Fig. 3E**) or between the ratio

239   of IgG1 to IgG4 (**Fig. S2A**). In the cohort receiving the bivalent vaccine, there was a similar trend

240   between the 2nd and 3rd vaccine but the additional WT/BA.1 mRNA vaccination had no impact on

241   ADCC activity despite small increases in Spike-specific IgG4 levels, suggesting a homeostatic limit to

242   the amount of ADCC (**Fig. 3F**).

243   Next, we compared the ability of plasma collected following 2nd and 3rd dose of BNT162b2

244   vaccine to stimulate antibody-dependent complement deposition (ADCD) and antibody-dependent

245   cellular phagocytosis (ADCP). As ADCD requires a complement source lacking antibodies to the

246   SARS-CoV-2 Spike, we utilised Guinea Pig complement serum that was naïve to SARS-CoV-2 Spike

247   (Polycarpou, 2023). Comparing ADCD activity in plasma post 2nd and 3rd dose showed a 3-fold increase

248   in the level of complement deposition (**Fig. 3G**). There was a positive correlation between ADCD

249   activity and IgG1 level, but no correlation was observed with IgG4 (**Fig. 3H**). ADCP activity was

250   measured using differentiated THP-1 cells as the effector cells and fluorescent beads coated with

251   recombinantly expressed SARS-CoV-2 Spike (Zohar et al., 2022). A 1.8-fold increase in ADCP activity

252   was observed following the 3rd mRNA vaccine (**Fig. 3J**). Similar to ADCD activity, there was a positive

253   but weak correlation between ADCP activity and IgG1 level, but no correlation was observed with IgG4

254   (**Fig. 3K**). Following administration of the bivalent booster, ADCD and ADCP levels remained

255   unchanged which is consistent with the smaller increase in Spike-specific IgG levels post bivalent

256   booster (**Fig. 3I and 3L**).

257   A previous study reported a decrease in ADCD and ADCP following a third dose of BNT162b2

258   mRNA vaccine (Irrgang et al., 2023), however, in these experiments the serum input was normalised to

259   the amount of Spike-specific Total IgG at each timepoint. When the ADCC, ADCD and ADCP activity

260   measured in our experiments was normalised to the amount of Spike-specific Total IgG, we also

261   observed a decrease in ADCD, and ADCP, as well as ADCC, for the Post3 samples compared to Post2

262   samples suggesting increasing IgG4 may limit effector function activity (**Fig. S2B**). No significant

263   difference was observed for neutralisation. Nevertheless, given that there are increases in all IgG

264   subclasses between Post2 and Post3 (**Fig. 1B**), the absolute ability of serum to activate these effector

265   functions would be most physiologically relevant, rather than the relative functional ability.

266   In summary, between the 2nd and 3rd mRNA vaccine doses, where there is a 3.2-fold increase

267   in IgG1 and an ~100-fold increase in IgG4, we observe increased neutralisation, ADCD and ADCP in

268   the plasma of individuals in the extended group. However, despite ADCC activity correlating with IgG1

269 concentration, ADCC activity in plasma does not increase significantly suggesting Spike-specific IgG4

270 impacts effector function activities differently.

271

272 **IgG4 maintains neutralisation activity, but loses Fc-dependent effector functions**

273 Next, we investigated the specific contribution that IgG4 makes to the effector function activity

274 measurements. Due to the technical challenges in separating the different subclasses of Spike-specific

275 IgG from plasma we recombinantly expressed IgG1, IgG2, IgG3 and IgG4 versions of a panel of SARS-

276 CoV-2 specific mAbs previously isolated from infected or vaccinated individuals (Graham et al., 2021;

277 Seow et al., 2022). mAbs were selected based upon their ability to activate degranulation of CD16

278 expressing NK cells in the ADCC assay (**Fig. S3**). mAbs selected targeted several different epitopes on

279 Spike. P008_60 is SD1 specific (Graham et al., 2021), P008_87 is a Class 3 RBD-specific mAb that

280 binds an epitope on the outer face of RBD (Graham et al., 2021), VA14_1 and VA14_R39 are Class 4

281 RBD-specific mAbs that bind the interior face of RBD (Seow et al., 2022), and P008_99 is NTD-

282 specific (Graham et al., 2021) (**Fig. S3A**). Note that none of the RBD Class 1 specific mAbs that bind

283 the ACE2 receptor binding site were able to facilitate ADCC.

284 We first investigated the ability of immune complexes containing the different subclasses of

285 IgG to bind to Fc receptors on the surface of various immune cells. NK cells express CD16 (FcγRIIIa),

286 and incubation of mAb-immune complexes with NK cells demonstrated similar binding of IgG1 and

287 IgG3 antibodies, but very low binding of the IgG2 and IgG4 subclasses (**Fig. S4A**). Raji cells expressing

288 CD32 (FcγRIIa and FcγRIIb) (Cassel et al., 1993), bound immune complexes of all subclasses equally

289 (**Fig. S4B**). THP-1 cells differentiated using PMA and IFNγ express both CD32 (FcγRII) and CD64

290 (FcγRI) (Fleit and Kobasiuk, 1991), and these showed weaker binding of IgG4 compared with other

291 subclasses (**Fig. S4C**). Given that there was no difference in binding to Raji cells expressing CD32

292 alone, the difference in binding to the differentiated THP-1 cells is likely due to reduced binding

293 between CD64 and the IgG4 Fc region.

294   Neutralisation of virus by IgG is largely antibody Fc-binding independent (Mozdzanowska et

295   al., 2003), and indeed, class-switching each of these SARS-CoV-2 mAbs to IgG1, IgG2, IgG3 and IgG4

296   had no impact on their ability to neutralise ancestral SARS-CoV-2 pseudovirus infection of HeLa-ACE2

297   cells (**Fig. 4A**). Having demonstrated unchanged neutralisation activity, we next measured effector

298   function activities of the class-switched antibodies. For all five mAbs, the IgG1 and IgG3 subclasses

299   were able to stimulate CD16 expressing NK-92 cells to degranulate in the ADCC assay as measured by

300   CD107a cell surface expression (Bartsch et al., 2023) (**Fig. 4B**). However, IgG2 and IgG4 subclasses

301   were not able to activate degranulation of these cells, consistent with their inability to bind to the CD16

302   expressing NK-92 cell line (**Fig. S4A**).

303   In the complement activation assay, IgG1 and IgG3 versions of P008_87 were equally able to

304   fix complement C3, and IgG2 and IgG4 displayed an 8-fold and 100-fold reduced complement fixation

305   activity, respectively, when Spike was coated at 3 mg/mL (**Fig. 4C**). When the complement deposition

306   assay was repeated with concentrated virus like particles (VLPs) expressing SARS-CoV-2 Spike coated

307   on the ELISA plate, no ADCD activity of IgG4 could be detected (**Fig. 4D**) presumably due to a lower

308   avidity of C3q binding. This hypothesis was confirmed, as ADCD activity of the IgG4 mAbs was also

309   absent when the recombinant Spike was coated at a lower density of 0.3 mg/mL (**Fig. 4E**). A similar

310   trend was observed for the remaining IgG4 mAbs on both concentrated VLPs (**Fig. S5**) and recombinant

311   Spike coated at 0.3 mg/mL (**Fig. 4F**).

312   Finally, in the ADCP assay, equal phagocytic activity was observed for the IgG1, IgG2 and

313   IgG3 subclasses of each mAb, but a 5 to 15-fold reduction in the phagocytic activity of IgG4 which is

314   consistent with the reduced binding to the differentiated THP-1 cells (**Fig. 4G**). Overall, the IgG4

315   subclasses were unable to facilitate ADCC and had reduced ADCD and ADCP activity.

316

317   **Non-competing IgG4 is functionally silent, not inhibitory**

318   Antibodies function *in vivo* within a polyclonal mix of antigen-specific antibodies of different

319   isotypes and subclasses. To determine the functional impact of Spike-specific IgG4 on overall antibody

320   effector function of plasma, we next investigated how the mAbs of different IgG subclasses, either

321   targeting the same epitope or non-competing epitopes, would interact with one another in effector

322   function assays.

323   First, we investigated the effect of the presence of IgG4 targeting the same epitope as an IgG1

324   with potent ADCC activity. We maintained a constant level of the IgG1 version of the mAb (either

325   P008_87 or VA14_R39), prior to titrating in either additional IgG1 or IgG4 of the same mAb. Adding

326   in additional IgG1 of the mAb led to an increased NK cell degranulation once the concentration was

327   greater than the baseline level of mAb (**Fig. 5A**). However, addition of the IgG4 version of the mAb

328   binding to the same epitope led to inhibition of degranulation, likely due to competition for binding to

329   a shared epitope on Spike. The same trend was observed for both P008_87 and VA14_R39. However,

330   this inhibition of ADCC activity was not observed when an IgG4 targeting a non-competing epitope

331   was added (**Fig. 5B**). Again, a constant level of IgG1 antibody was maintained, but either an additional

332   IgG1 or IgG4 of a non-competing mAb was added. Addition of IgG1 similarly led to additional NK cell

333   degranulation. However, addition of IgG4 as a non-competing antibody had no effect on overall

334   degranulation. A similar experimental approach was used to study the direct impact of Spike-specific

335   IgG4 on ADCD by a potent IgG1 mAb. When IgG1 was added to a constant level of IgG1 targeting the

336   same epitope (either P008_87 or VA14_R39), an increase in ADCD was observed when the IgG4

337   version of this mAb was added a decrease in ADCD indicating an inhibitory effect (**Fig. 5C**). However,

338   addition of an IgG1 or IgG4 targeting a different Spike epitope, showed no decrease in ADCD activity

339   (**Fig. 5D**). Overall, the presence of Spike specific IgG4 could potentially decrease effector function

340   activity (both ADCC and ADCP) through preventing the binding of IgG subclasses that are potent

341   activators of effector functions, including IgG1.

342   To determine whether such an effect might be seen *in vivo* in the context of a polyclonal

343   antibody response, we added a cocktail of the five IgG4 mAbs targeting different Spike epitopes to

344   plasma collected after two mRNA doses where Spike-specific IgG4 level is very low and measured the

345   impact on ADCD and ADCC (**Fig. S6A-B**). Pooled IgG4 or IgG1 was added at a combined

346   concentration of 1 mg/mL, which greatly exceeds the maximum level of Spike-specific IgG4 measured

14

347   in plasma. Addition of pooled Spike-specific IgG1 mAbs was able to increase the level of ADCD and

348   ADCC (**Fig. S6A** and **S6B**). However, although the pooled IgG4 was able to compete the activity of

349   IgG1 mAb P008_99 (**Fig. S6A** and **S6B**), no difference in ADCD or ADCC activity was observed for

350   the polyclonal plasma. This difference may be due to the recombinant IgG4s only targeting a proportion

351   of the potential Spike epitopes targeted by the functional IgG1 and IgG3 in the polyclonal plasma. These

352   data suggest that the interplay between IgG1 and IgG4 within the context of the polyclonal sera where

353   there is a wider array of neutralising and non-neutralising epitopes targeted on Spike, is more complex.

354

Discussion

356   This study supports previous observations that the COVID-19 mRNA based vaccine,

357   BNT162b2, can lead to a Spike-specific IgG4 response following multiple exposures (Akhtar et al.,

358   2023; Buhre et al., 2022; Gelderloos et al., 2024; Irrgang et al., 2023). This study extends these

359   observations further through additional understanding of the factors impacting switch to IgG4 following

360   BNT162b2 vaccination and the functional activity and potential consequences of high levels of Spike-

361   specific IgG4.

362   Comparing the kinetics and magnitude of Spike-specific IgG4 production in individuals with

363   varying vaccination histories enabled us to identify additional factors that impact IgG4 class-switching

364   in the context of mRNA vaccination. The interval between first and second BNT162b2 dose proved

365   important for the switch to Spike-specific IgG4 as demonstrated by an elevated level of IgG4 in the

366   extended (12-week interval) vs short (3-week interval) group at 6-months post second vaccine dose.

367   However, a third BNT162b2 dose resulted in boosting to reach similar levels of Spike-specific IgG4 in

368   both the short and extended groups. This data suggests that vaccine interval alone is not sufficient to

369   explain the previously reported difference in production of Spike-specific IgG4 between BNT162b2

370   administered at a 3-week interval and AZD1222 administered at a 12-week interval, where no Spike-

371   specific IgG4 was detected, but the difference must also be related to the vaccine type and formulation

372   (Hartley et al., 2024). We observed the level of Spike-specific IgG4 to further increase following

15

373   additional mRNA vaccination similar to Gelderloos *et al* who showed that the IgG4 level can continue

374   to increase after up to 5-doses of mRNA vaccine in older adults (Gelderloos et al., 2024). Spike antigen

375   exposure through breakthrough infection also increased IgG4 Spike levels. Whether these increases are

376   due to continued evolution of already switched IgG4 or due to new class-switching events needs to be

377   investigated. However, the class-switch to IgG4 is specific for SARS-CoV-2 Spike in the form of an

378   mRNA-based immunogen as Nucleoprotein-specific IgG4 was not detected following two SARS-CoV-

379   2 breakthrough infections, and HA-specific IgG4 was not detected in individuals co-immunised with

380   the influenza vaccine at the time of mRNA booster vaccination. These results indicate there may be

381   specific conditions created by the mRNA vaccine that make B cells more prone to induce class switch

382   recombination (CSR) to distal subclasses. Investigation of class-switching to antigen-specific IgG4 for

383   other mRNA-based vaccines is required.

384   It has been proposed that long germinal centre reactions observed following mRNA

385   vaccination, where there is a prolonged presence of the Spike antigen in the lymph node (Kim et al.,

386   2022; Roltgen et al., 2022; Turner et al., 2021), might explain the high-level of Spike-specific IgG4

387   (Irrgang et al., 2023). Prolonged antigen exposure has been proposed as the mechanism behind

388   generation of IgG4 responses to honey bee venom observed in bee keepers (Aalberse et al., 1983).

389   However, prolonged antigen exposure through repeated vaccination with tetanus vaccines is not

390   sufficient to generate a vaccine specific IgG4 response (Unger et al., 2018). Furthermore, despite

391   continued maturation of the Spike-specific IgG response being observed for at least 6-months post

392   SARS-CoV-2 infection, presumably due to extended antigen exposure (Gaebler et al., 2021), no Spike-

393   specific IgG4 was detected in our longitudinal infection cohort, including both mild and severe disease,

394   up to 33 weeks post infection. These observations highlight that repeated or prolonged antigen exposure

395   is not sufficient to facilitate IgG4 switch.

396   The distribution in IgG4-binding to the RBD and NTD domains was similar to that observed

397   for total IgG and IgG1 suggesting there is no epitope bias in the subclass switching. As the IgG4 shows

398   a similar breadth of variant Spike binding it also suggests that the IgG4 B cells could be arising from

399   re-activation and switching of existing Spike-reactive B cells rather than a *de novo* response.

16

400 Additionally, SARS-CoV-2 infection prior to BNT162b2 vaccination was observed to accelerate the

401 appearance of Spike-specific IgG4, with IgG4 first being detected at low levels from 3 weeks post 1st

402 BNT162b2 dose in 3/8 individuals and in all (8/8) individuals from 3 weeks post 2nd dose. This more

403 rapid appearance suggests that IgG subclasses generated in response to SARS-CoV-2 infection can be

404 class-switched to IgG4 upon mRNA vaccination indicative of reactivation of existing B cell clones

405 rather than generation of a *de novo* response. However, it is noteworthy that the avidity of the Spike-

406 specific IgG4 lags behind that of the Total-IgG, particularly against the BA.1 variant Spike. In contrast

407 to the former observation, this may indicate that IgG4 production does not primarily arise from the

408 class-switching of high avidity IgG subclasses. Alternatively, the lower avidity could also arise due to

409 the ability of IgG4 to undergo Fab arm exchange leading to monovalent antibody binding with reduced

410 avidity (van der Neut Kolfschoten et al., 2007). Further investigations into the clonal origin of IgG4 in

411 relation to other antibody classes and IgG subclasses over time is required to understand the origin of

412 IgG4 further.

413 Antibody effector functions have been shown to be important in the therapeutic and

414 prophylactic activity of SARS-CoV-2 mAbs in animal models (Gorman et al., 2021; Zhang et al., 2023).

415 A significant concern with the elicitation of Spike-specific IgG4 is the reported anti-inflammatory

416 properties arising from reduced affinity to Fcγ receptors (Pillai, 2023; Vidarsson et al., 2014).

417 Importantly, despite the production of Spike-specific IgG4, repeated mRNA vaccine boosting has

418 remained protective from severe COVID-19 (Lee et al., 2023). The consequence of high levels of Spike-

419 specific IgG4 on effector function activity is difficult to tease apart due to the polyclonal nature of

420 plasma, and the varying proportions and amounts of Spike-specific IgG1, IgG2, IgG3 and IgG4 both at

421 different timepoints and between individuals, as well as the lack of animal models that produce IgG4

422 (Olivieri and Gambon Deza, 2018). By isotype-switching previously characterised Spike-specific

423 mAbs, we have been able to investigate the functional implications of elevated levels of Spike-specific

424 IgG4 more directly. As expected, antibody class-switching had no impact on the ability of mAbs to

425 neutralise SARS-CoV-2 which is consistent with the increasing plasma neutralising activity observed

426 as Spike-specific Total IgG increases. Spike-specific IgG1 and IgG3 were able to facilitate ADCC,

17

427   ADCD and ADCP equally. Spike-specific IgG2 lost ADCC activity, retained ADCP activity and was a

428   weak activator of ADCD. Spike-specific IgG4 had the lowest levels of effector function activity,

429   showing no ADCC and ADCD activity (at low antigen densities) and had a 10-fold reduction in ADCP.

430   Using mAbs expressed as different subclasses in ADCC and ADCD competition assays, we showed

431   that in the context of viral infection the Spike-specific IgG4 is functionally silent unless there is direct

432   binding competition with a functionally active IgG1. In this scenario the IgG4 reduces effector function

433   activity by preventing the binding of IgG1 to the Spike antigen. In the context of allergy, increased titres

434   of allergen specific IgG4 has been shown to reduce hypersensitivity through blocking the activity of

435   IgE (Santos et al., 2015) and IgG4 in the context of mRNA vaccination may have a comparative function

436   in reducing inflammatory responses whilst maintaining the ability to neutralise free virus. Indeed, this

437   blocking nature of IgG4 makes it a commonly used format for therapeutic monoclonal antibodies due

438   to its limited ability to induce inflammatory responses (Rispens and Huijbers, 2023). Despite the

439   unusual presence of Spike-specific IgG4, the relatively low-level present compared to the more

440   functionally active IgG1 suggests the inhibitory effect arising from steric occlusion could be out-

441   competed for the limited antigenic sites on the surface of a virion or infected cell or the lower avidity

442   of IgG4 binding. Furthermore, in the context of SARS-CoV-2 infection, antibodies against viral proteins

443   other than Spike can also mediate effector functions such as ADCC (Fielding et al., 2022). Therefore,

444   the non-stimulatory effect of Spike-specific IgG4 may be hidden in more complex scenarios, such as

445   polyclonal mixes. Indeed, we were unable to inhibit ADCD or ADCC activity in polyclonal sera through

446   addition of a cocktail of Spike-specific IgG4s at high concentrations (up to 1 mg/mL).

447   In summary, we show that factors including vaccine interval and frequency, hybrid immunity

448   and breakthrough infection all enhance the production of Spike-specific IgG4 following BNT162b2

449   mRNA vaccination. Through generation of Spike-specific mAbs of each IgG subclass, we showed that

450   the IgG4 can inhibit ADCC and ADCD activity of potently activating IgG1 through direct binding

451   competition. However, the polyclonal nature of plasma and the lower avidity of IgG4 binding observed

452   suggest that the impact on overall effector function activity is likely to be minimal, and will be heavily

453   dependent on the epitope specificity of the IgG4 antibodies produced. Further research is needed to

454 understand the factors that trigger IgG4 class switching in the context of mRNA vaccination and the

455 origin of the antigen-specific IgG4 antibodies.

456

457 **Materials and methods**

458 **Volunteer Samples/Ethics**

459 Demographics of the vaccinated and infected volunteer samples are shown in **Supplementary Table**

460 **1**. Samples were collected according to the timeline shown in **Supplementary Fig. S1**. This study used

461 human samples collected with written consent as part of a study entitled "Antibody responses following

462 COVID-19 vaccination." Ethical approval was obtained from the King's College London Infectious

463 Diseases Biobank (IBD) (KDJF-110121) under the terms of the IDB's ethics permission (REC

464 reference: 19/SC/0232) granted by the South Central Hampshire B Research Ethics Committee in 2019

465 and London Bridge Research Ethics Committee (reference: REC14/LO/1699). Collection of surplus

466 serum samples at St Thomas Hospital, London, was approved by South Central-Hampshire B REC

467 (20/SC/0310).

468 **Bacterial Strains and Cell Culture**

469 SARS-CoV-2 pseudotypes were produced by transfection of HEK293T/17 cells (ATCC CRL-11268)

470 and neutralisation activity assayed using HeLa cells stably expressing ACE2 (kind gift from Dr James

471 Voss, Scripps Research, CA). Monoclonal antibodies were expressed in HEK293 Freestyle (HEK293F)

472 cells (Thermofisher Scientific). NK-92 cells (obtained from ATCC, CRL-2407) transduced with high

473 affinity (Valine 158) human CD16, THP-1 (TIB-202) and Raji (CCL-86) cells were obtained from

474 ATCC. HEK293T/17 cells and HeLa-ACE2 cells were maintained in Dulbecco's Modified Eagle

475 Medium supplemented with GlutaMAX, 10% Foetal Calf Serum and 1% Penicillin/Streptomycin

476 (DMEM-C). HEK293F cells were maintained in Freestyle media. THP-1 and Raji cells were maintained

477 in Roswell Park Memorial Institute (RPMI) 1640 supplemented with GlutaMAX, 10% Foetal Calf

478 Serum (RPMI-C). NK-92 cells expressing CD16 were maintained in Minimum Essential Medium α

479 (MEM α) supplemented with L-glutamine, nucleosides, 12.5% Foetal Calf Serum, 12.5% Horse Serum,

480 20mM HEPES, 0.2mM Myo-inositol, 0.02mM Folic Acid, 0.1mM 2-mercaptoethanol and 50IU/ml

481 Interleukin (IL)-2. Bacterial transformations for class switching were performed with NEB Stable

482 Competent *E.coli*.

Protein Expression and Purification

484 Recombinant Spike, RBD and NTD (residues 1-310) were expressed and purified as previously

485 described (Rosa et al., 2021; Seow et al., 2020). Recombinant SARS-CoV-2 WT Nucleocapsid (N

486 protein) was a kind gift from Dr Leo James, Laboratory of Molecular Biology, Cambridge.

487 Recombinant Spike trimers were engineered from full-length Spike expression plasmids (pcDNA3.1

488 plasmid) using a molecular cloning approach. The furin cleavage site (RRAR) was replaced with a

489 flexible linker (GGGG), and the K986 and V987 residues in the S2 subunit were mutated to prolines

490 using site-directed mutagenesis. The resulting sequences were truncated at amino acid position 1138

491 and subcloned into pHLSec (Aricescu et al., 2006) via Gibson assembly, positioning them upstream of

492 a flexible linker (GSGG), T4 foldon trimerisation domain, and incorporating Avi and His tags.

493 Biotinylated Spike was expressed as previously described (Graham et al., 2021). Biotinylated Spike

494 was expressed in 1L of HEK293F cells (Invitrogen) at a density of 1.5×10^6 cells/mL. To achieve *in*

495 *vivo* biotinylation, 480μg of each plasmid was co-transfected with 120μg of BirA (Howarth et al., 2008)

496 and 12mg PEI-Max (1 mg/mL solution, Polysciences) in the presence of 200 μM biotin (final

497 concentration). The supernatant was harvested after 7 days and purified using immobilised metal

498 affinity chromatography and size-exclusion chromatography. Complete biotinylation was confirmed

499 via depletion of protein using avidin beads.

500 Influenza HA haemagluttinin A/California 04/2009 was cloned into the pHLSec vector containing a

501 6xHIS tag, and expressed and purified in the same manner as for SARS-CoV-2 Spike.

IgG subclass cloning and expression

503 SARS-CoV-2 monoclonal antibodies were isolated and characterised previously (Graham et al., 2022;

504 Seow et al., 2022). Heavy chains were PCR amplified using previously described primers and

505 conditions (Graham et al., 2022; Seow et al., 2022; Tiller et al., 2008), and cloned into human IgG

506   heavy chains of IgG2 (Addgene AbVec2.0-IGHG2 #99576), IgG3 (AbVec2.0-IGHG3 #99577) and

507   IgG4 (AbVec2.0-IGHG4 #99578) using the Gibson Assembly Master Mix (NEB) following the

508   manufacturer's protocol. AbVec2.0-IGHG2, AbVec2.0-IGHG3 and AbVec2.0-IGHG4 were a gift from

509   Hedda Wardemann (Addgene plasmid #99576, #99577 and #99578; RRID:Addgene_99576,

510   RRID:Addgene_99577 and RRID:Addgene_99578).

511   Ab heavy and light plasmids were co-transfected at a 1:1 ratio into HEK-293F cells (Thermofisher)

512   using PEI Max (1 mg/mL, Polysciences, Inc.) at a 3:1 ratio (PEI Max:DNA). Ab supernatants were

513   harvested five days following transfection, filtered and purified using protein G affinity

514   chromatography following the manufacturer's protocol (GE Healthcare).

515   **Pseudovirus production**

516   HEK293T/17 cells were seeded in a 10cm dish at a density of 3×10^5cells/mL. Following overnight

517   culture, cells were co-transfected using 90 μg PEI-Max (1 mg/mL, Polysciences) with 15 μg HIV-

518   luciferase plasmid, 10 μg HIV 8.91 gag/pol plasmid, and 5 μg SARS-CoV-2 Spike protein plasmid

519   (Zufferey et al., 1997). Transfected cells were incubated for 72 h at 37°C, and virus was harvested,

520   sterile filtered, and stored at −80°C until required.

521   **VLP production and quantification**

522   HEK293T/17 cells were seeded in a 10cm dish at a density of 3×10^5 cells/mL. Cells were transfected

523   using 90μL PEI with the following plasmids: 2.5μg WT SARS-CoV-2 Spike plasmid, 8μg HIV gag/pol

524   mScarlet plasmid, 2μg HIV 8.91 gag/pol plasmid, and 10μg HIV-luciferase plasmid. The supernatant

525   containing the VLPs was collected 72h post-transfection, clarified by centrifugation at 3000×g for 15

526   min and passed through a 0.45μm filter. The clarified supernatant was then layered onto a sucrose

527   cushion (20% sucrose, 50 mM Tris-HCl, 0.5 mM EDTA, and 100 mM NaCl in PBS, pH 7.4) and

528   centrifuged at 10000×g for 4h at 4°C. The supernatant was gently aspirated and the concentrated VLPs

529   were resuspended in PBS. The samples were then stored at -80°C until use. Infectivity of VLPs was

530   measured using HeLa ACE2 cells.

531   **Antibody Subclass ELISA**

532 High-binding ELISA plates (Corning, 3690) were coated with antigen (N protein, S glycoprotein, RBD,

533 NTD or Influenza HA) at 3 μg/mL (25 μl per well) in phosphate-buffered serum (PBS) overnight at 4

534 °C. Wells were washed with PBS-T (PBS with 0.05% Tween-20) and then blocked with 100 μl of 5%

535 milk in PBS-T for 1 h at room temperature. The wells were emptied, and serial dilutions of plasma

536 (heat-inactivated at 56°C for 30 min) were added and incubated for 1 h at room temperature. Dilutions

537 of a known monoclonal antibody standard, and serum antibody standard ERM-DA470k (Sigma)

538 (Wilson et al., 2013) were used for quantification. Wells were washed with PBS-T. Secondary

539 antibodies were added (1:1000 dilution in 5% No Fat Milk in PBS-T) and incubated for 1 h at room

540 temperature, including goat-anti-human Total IgG-alkaline phosphatase (AP) (Jackson

541 Immunoresearch, 109-055-098), mouse-anti-human IgG1-horseradish peroxidase (HRP) (Invitrogen

542 A10648), mouse-anti-human IgG2-HRP (Invitrogen MH1722), mouse-anti-human IgG3-HRP

543 (Southern Biotech 9210-05), mouse-anti-human IgG4-HRP (Invitrogen MH174225)). Wells were

544 washed with PBS-T and either AP substrate (Sigma) was added and read at 405 nm (AP) or one-step

545 3,3′,5,5′-tetramethylbenzidine (TMB) substrate (Thermo Fisher Scientific) was added and quenched

546 with 0.5 M H_2S0_4 before reading at 450 nm (HRP). Quantification was conducted by comparing

547 dilutions to reach the same EC_{50} value calculated by GraphPad Prism.

548 **Avidity Assay**

549 The avidity ELISA was carried out as described above except for one additional step. After incubation

550 of plasma, one half of the plate was incubated with 8M Urea and the other half incubated with PBS for

551 15 min before washing 5-times with PBS-T. The area under the curve was determined in Prism (Log

552 dilution). The avidity index was calculated using the following formula:

553 $$Avidity\ index = 100 * \left(\frac{Area\ under\ curve\ with\ 8M\ Urea}{Area\ under\ curve\ with\ no\ Urea} \right)$$

554 **Immune Complex Binding Assay**

555 NK-92 cells expressing human CD16, THP-1 cells and Raji cells were plated at $1.0x10^5$ cells/well on

556 high-binding full-well 96 well plates. Immune complexes were formed by incubating 25μl of serially

22

557   diluted mAb in RPMI-C (at concentrations stated), with WT Spike protein (25µl at 3.0 µg/ml) for 1h.

558   Immune complexes were then incubated with each cell type for 1h. Cells were then washed with PBS-

559   T, and blocked with Fc Block (BD Biosciences) for 1h. Following a final was in PBS-T, binding to cells

560   was measured using the same secondary antibodies as for ELISA above.

Neutralisation Assay

562   Serial dilutions of plasma samples (heat inactivated at 56°C for 30mins) or monoclonal antibody were

563   prepared in DMEM-C (to total 25µL) and incubated with pseudotyped virus (25µL) for 1h at 37°C in

564   half-area 96-well plates. HeLa ACE2 cells were diluted to a concentration of $5x10^5$cells/mL and added

565   to each well (25µL/well), and plates incubated at 37°C for 72h. Infection levels were quantified by

566   lysing the cells and measuring luciferase activity using the Bright-Glo Luciferase Assay Kit (Promega)

567   on a Victor X3 multilabel plate reader (PerkinElmer).

Antibody Dependent Cellular Cytotoxicity (ADCC) Assay

569   ADCC assay was adapted from Bartsch *et al* (Bartsch et al., 2023). High-binding full-well ELISA plates

570   were coated with Spike protein at 3 µg/mL (50 µl per well) in PBS for 2h at 37 °C. Wells were washed

571   with PBS and then blocked with 100 µl of 5% bovine serum albumin in PBS overnight at 4°C. The

572   plates were then washed with PBS, prior to addition of serial dilutions of heat inactivated plasma

573   samples or monoclonal antibody diluted in DMEM-C and incubated at room temperature for 1h. NK-

574   92 CD16 cells were added ($1.0x10^5$cells/well) in media supplemented with an increased IL-2

575   concentration (100 IU/ml), Golgistop protein transport inhibitor (BD Biosciences #554724, 5µl per

576    $1.0x10^6$cells) and PerCP/Cyanine5.5 anti-human CD107a antibody (Biolegend Clone H4A3). Plates

577   were incubated at 37°C , 5% CO_2 for 6h. NK-92 cells were transferred to 75mm Polystyrene Tubes,

578   washed with PBS and fixed by addition of 4% paraformaldehyde. Level of CD107a surface expression

579   was measured by flow cytometry using a BD Canto II.

Antibody Dependent Complement Deposition (ADCD) Assay

581   ADCD assay was adapted from Ref (Polycarpou, 2023). High-binding ELISA plates (Corning, 3690)

582   were coated with Spike protein at 3 µg/mL or 0.3 µg/mL (25 µl per well) in phosphate-buffered serum

23

583 (PBS) overnight at 4 °C. For VLP assays, purified VLPs at 4×10^6 infectious units/well were incubated

584 at room temperature for 2h. Wells were washed with PBS-T (PBS with 0.05% Tween-20) and then

585 blocked with 100 μl of 5% milk in PBS-T for 1h at room temperature. Serial dilutions of heat-

586 inactivated plasma or mAbs (25μl in PBS) were added and incubated for 1h at room temperature,

587 followed by washing with PBS-T. Guinea Pig Complement Serum (Sigma S1639) was diluted to 1:100

588 (as per the complement activity level) in HEPES Buffered Saline (0.01 M HEPES, 0.15 M NaCl,

589 135 nM $CaCl_2$, 1 mM $MgCl_2$, adjusted to pH 7.4) as barbitone buffers are not available (Zelek et al.,

590 2018). Diluted complement was added to the wells, alongside a heat inactivated control plasma (56°C

591 for 30mins), and plate was incubated for 1h. Wells were washed with PBS-T, prior to addition of Goat

592 Anti-Guinea Pig Complement C3 polyclonal (1:250 in 5% milk/PBS-T, MP Biomedicals 0855371) for

593 1h at room temperature. Wells were washed with PBS-T, and incubated with HRP-conjugated Mouse

594 Anti-Goat IgG (1:500, Santa Cruz Biotechnology sc-2354). Wells were then washed and TMB substrate

595 added which was quenched with 0.5 M H_2SO_4 before reading at 450 nm (HRP).

Antibody Dependent Cellular Phagocytosis (ADCP) Assay

597 The ADCP assay was based on previously published protocol (Zohar et al., 2022). Briefly, biotinylated

598 SARS-CoV-2 Spike (5μL at 1 mg/mL) was incubated with 10μl of washed yellow-green fluorescent

599 NeutrAvidin-Labeled Microspheres (480-505nm, 1.0μm size, Thermofisher), and incubated at 37 °C

600 for 2h. Beads were washed twice (0.1% PBS-BSA) by centrifugation (16000xg, 5min) at room

601 temperature. The antigen-coupled fluorescent beads were resuspended in 0.1% PBS-BSA (1:500 by

602 volume). 2.5μl of this bead suspension was incubated with 5μl heat inactivated plasma or antibody

603 dilutions at room temperature for 1h. THP-1 cells (25,000/well) and bead/plasma mixes were added to

604 24 well plates and incubated for 16h at 37°C, 5% CO_2. Cells were washed and bead uptake measured

605 by flow cytometry using a BD FACS Canto II. Phagocytosis scores were determined by first plotting

606 the antibody concentration against the geometric mean fluorescence intensity of the bead positive THP-

607 1 cells multiplied by the percent of bead positive THP-1 cells. These curves were used to calculate the

608 AUC using GraphPad Prism.

**IgG Subclass ADCC and ADCD Competition Assays**

610   For competition assays, IgG1 of P008_87 or VA14_R39 were titrated to either 10% NK-92 cell

611   degranulation activity or 25% complement C3 detection (0.5 at 450nm absorbance). Further P008_87

612   or VA14_R39 of IgG1 or IgG4 subclass was then added into this antibody mixture at different serial

613   dilutions. These antibody mixes were then used in the ADCC and ADCD assays as described above.

614   **Plasma Spiked IgG4 Assay**

615   P008_60, P008-87, P008_99, VA14_1 and VA14_R39 IgG1 and IgG4 were pooled together for final

616   concentrations of 1 mg/ml each. The IgG4 mixture was serially diluted and 25uL added to plasma

617   samples (25µl of EC_{80} values calculated from a prior ADCD assay (roughly 1:100 dilution)). P008_99

618   IgG1 mAb was used at 1 µg/ml as an ADCD and ADCC positive control.

619

620

621

Figure 1
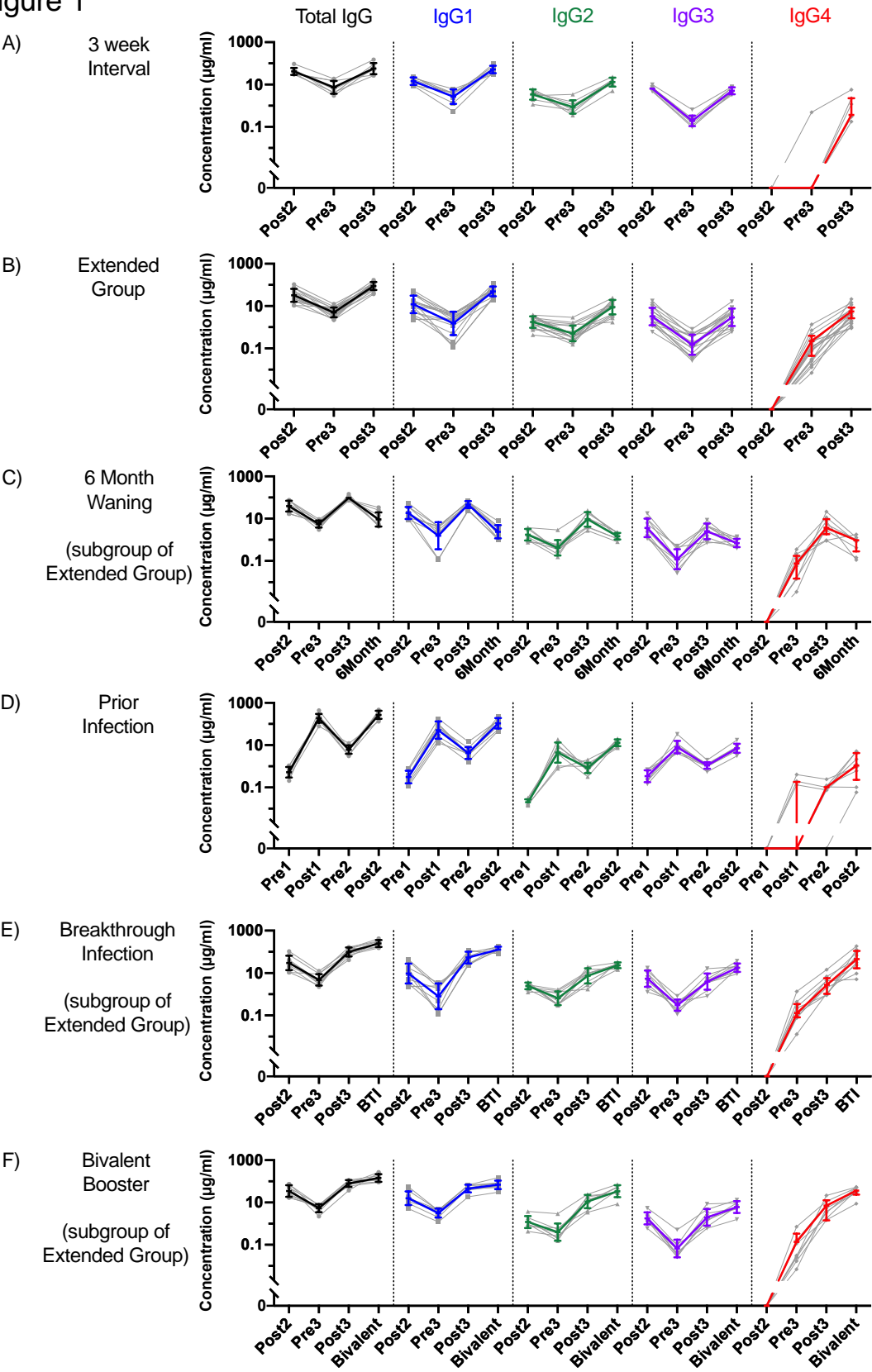
624 **Fig. 1** – **Spike-specific IgG4 production in individuals with different exposure histories.**

625 Semiquantitative ELISA measurement of Wildtype (WT) SARS-CoV-2 Spike-specific Total IgG

626 (black), IgG1 (blue), IgG2 (green), IgG3 (purple) and IgG4 (red) for **(A)** 3 week interval between 1st

627 and 2nd dose group (short group, n=8), **(B)** 12-week interval between 1st and 2nd dose group (extended

628 group, n=17), **(C)** subgroup of extended group with sample a 6 months post third dose (n=9), **(D)** prior

629 infection group (n=8), **(E)** subgroup of extended group with a breakthrough infection after three doses

630 (n=9), **(F)** subgroup of extended group with a bivalent WT/BA.1 booster 1 year after third dose (n=8).

631 Samples paired from an individual in grey with coloured data showing geometric mean and standard

632 deviation. Pre1 = before 1st dose, Post1 = 2 weeks after 1st dose, Pre2 = before 2nd dose, Post2 = 2 weeks

633 after 2nd dose, Pre3 = before 3rd dose, Post3 = 2 weeks after 3rd dose, 6Month = 6 month after 3rd dose,

634 BTI = 2 weeks after breakthrough infection, Bivalent = 2 weeks after bivalent dose. See Supplementary

635 Table 1 for demographics and Supplementary Fig. S1 for precise timings. Semiquantitative ELISA limit

636 of detection 0.05 μg/ml.

637

Figure 2

638
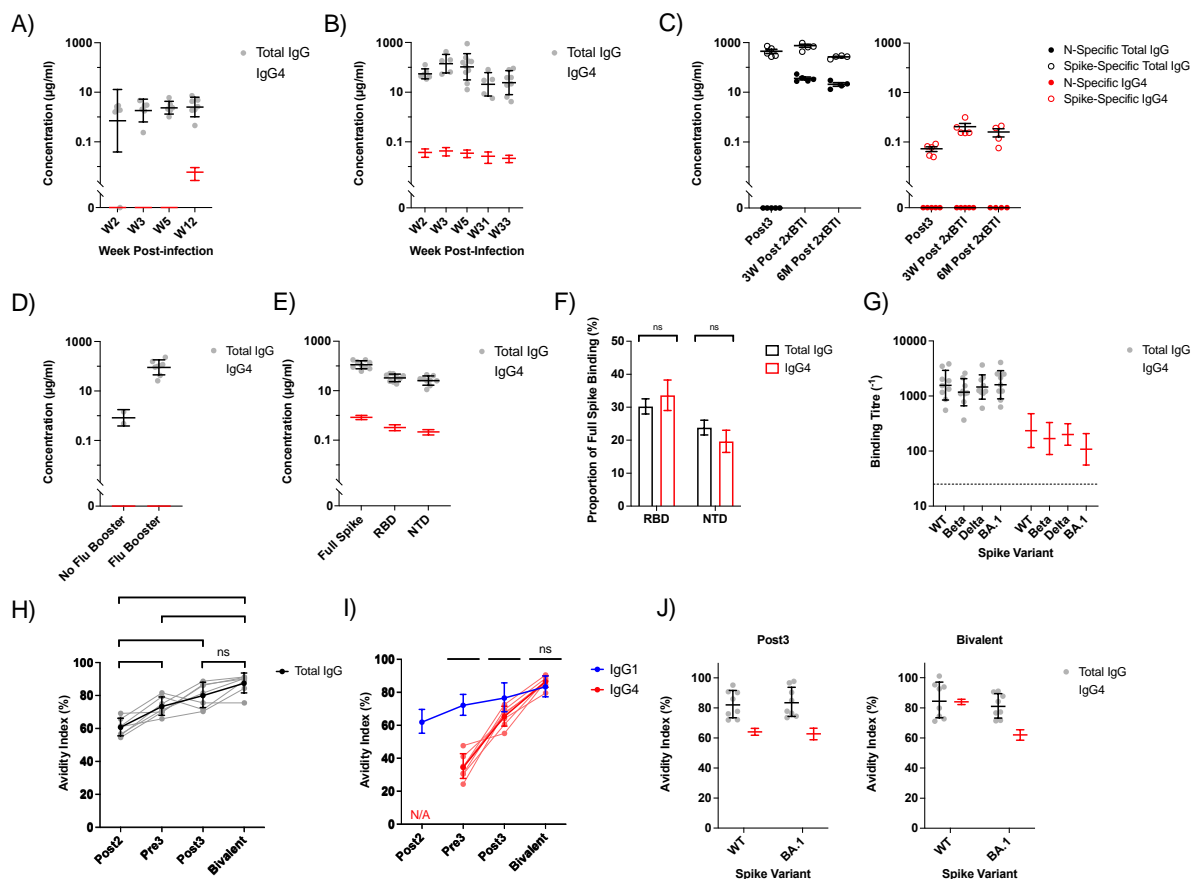
Fig. 2 –**Specificity and avidity of IgG4 arising from BNT162b2 mRNA vaccination.** Concentration of Spike-specific Total IgG (black/grey) and IgG4 (red/pink) in sera for **(A)** a mild infection group and **(B)** severe, ITU admission group. **(C)** Concentration of SARS-CoV-2 N-specific Total IgG (filled black circles), Spike-specific Total IgG (clear black circles), N-specific IgG4 (filled red circles), Spike-specific IgG4 (clear red circles), 2 weeks after 3rd dose (Post3), 3 weeks after 2nd breakthrough infection (3W Post 2xBTI) and 6 months after 2nd breakthrough infection (6M Post 2xBTI). **(D)** Concentration of Haemagglutinin-specific Total IgG (black/grey) or IgG4 (red/pink) with or without influenza booster given with 12-week interval 3rd Dose. **(E)** ELISA measurement of Total IgG (black/grey) and IgG4 (red/pink) targeted against WT SARS-CoV-2 Full Spike, Receptor-Binding Domain (RBD) and N-Terminal Domain (NTD) in 12-week interval Post3 samples. **(F)** RBD and NTD binding Total IgG (black) and IgG4 (red) as a proportion of binding to Full Spike. **(G)** Total IgG (black/grey) and IgG4 (red/pink) binding to WT, Beta, Delta and BA.1 Spike in 12-week interval Post3 samples. **(H)** Serum

651   antibody avidity of Total IgG (black) binding to WT Spike in Post2, Pre3, Post3 and Bivalent samples

652   from the Bivalent group. **(I)** As in (H), but for IgG1 (blue) and IgG4 (red). **(J)** Serum antibody avidity

653   of Total IgG (black/grey) and IgG4 (red/pink) against WT and BA.1 recombinant Spikes for Post3 and

654   Bivalent samples from the Bivalent group. In all panels, samples paired from an individual are in lighter

655   colour, with darker coloured data showing geometric mean and standard deviation. Data representative

656   of 3 technical replicates. ns=not significant, * $p<0.05$, ** $p<0.01$, *** $p<0.001$, **** $p<0.0001$

657

658

Figure 3

Fig. 3 – Functional activity of plasma with increasing Spike-specific IgG4. (A) Neutralising 50% Inhibitory Dose (ID_{50}) titre against WT SARS-CoV-2 Spike pseudotyped virus for 12-week interval Post2 and Post3 samples. **(B)** Correlation between Neutralising ID_{50} and IgG1 (blue) or IgG4 (red) concentration, with lighter colour for Post2 and darker colour for Post3 samples. **(C)** Neutralising ID_{50} titre for Bivalent group Post2, Post3 and Bivalent samples. **(D, E & F)** as (A, B & C) but for Antibody Dependent Cellular Cytotoxicity (ADCC) assay, measuring surface CD107a on activated NK cells. **(G, H & I)** as (A, B & C) but for Antibody Dependent Complement Deposition (ADCD) assay, measuring deposited C3. **(J, K & L)** as (A, B & C) but for Antibody Dependent Cellular Phagocytosis (ADCP) assay, measuring THP-1 macrophage uptake of WT Spike-coated fluorescent beads incubated with plasma. For all correlations, best fit line drawn for all IgG1 data, and include

670   data points with non-zero values of IgG4. The vertical dotted line represents the limit of IgG4

671   detection. Data representative of 3 technical replicates. ns=not significant, *** p<0.001

672

673

Figure 4
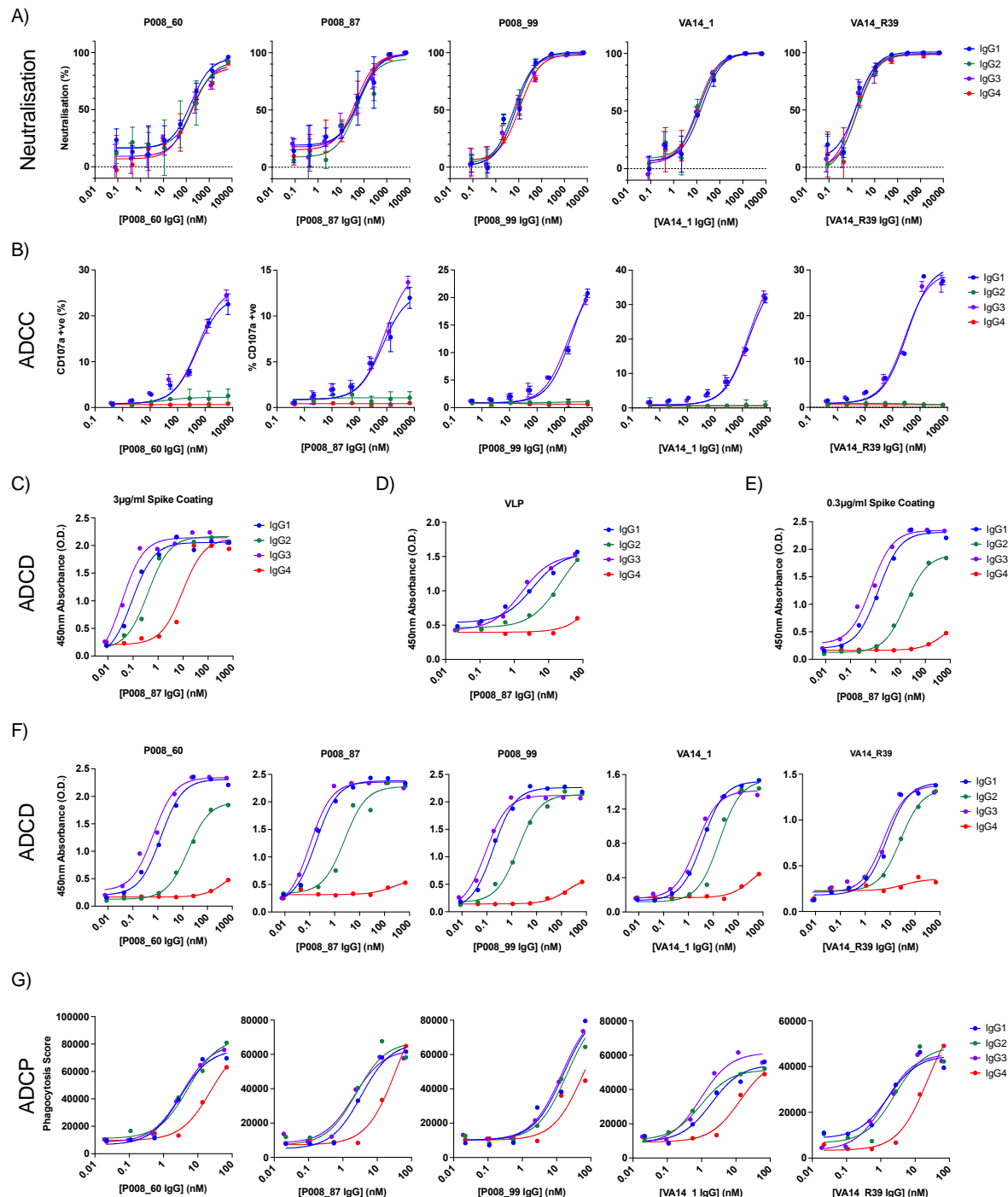
Fig. 4. **Functional activity of SARS-CoV-2 mAbs when expressed as different IgG subclasses.**

(A) Neutralisation curves for 5 monoclonal antibodies; P008_60, P008_87, P008_99, VA14_1, VA14_R39 class-switched to IgG1 (blue), IgG2 (green), IgG3 (purple) and IgG4 (red), against WT SARS-COV-2 Spike pseudotyped virus. **(B)** as in (A) but for ADCC measured as percentage of NK cells with surface-accessible CD107a. **(C)** ADCD assay for P008_87 as IgG1 (blue) or IgG4 (red)

680   with 3 μg/ml WT Spike ELISA plate coating. **(D)** ADCD assay for P008_87 as IgG1 (blue) or IgG4

681   (red) against Spike Virus-like Particles (VLP) (filled circles) or Naked VLPs (clear circles). **(E)**

682   ADCD assay for P008_87 as IgG1 (blue) or IgG4 (red) with 0.3 μg/ml WT Spike plate coating. **(F)**

683   ADCD for P008_60, P008_87, P008_99, VA14_1, VA14_R39 class-switched to IgG1 (blue), IgG2

684   (green), IgG3 (purple) and IgG4 (red) with 0.3 μg/ml WT Spike plate coating. **(G)** as in (A) but for

685   ADCP, measuring THP-1 macrophage uptake of WT Spike-coated fluorescent beads incubated with

686   antibody. Data representative of 3 technical replicates.

687

688

Figure 5

689
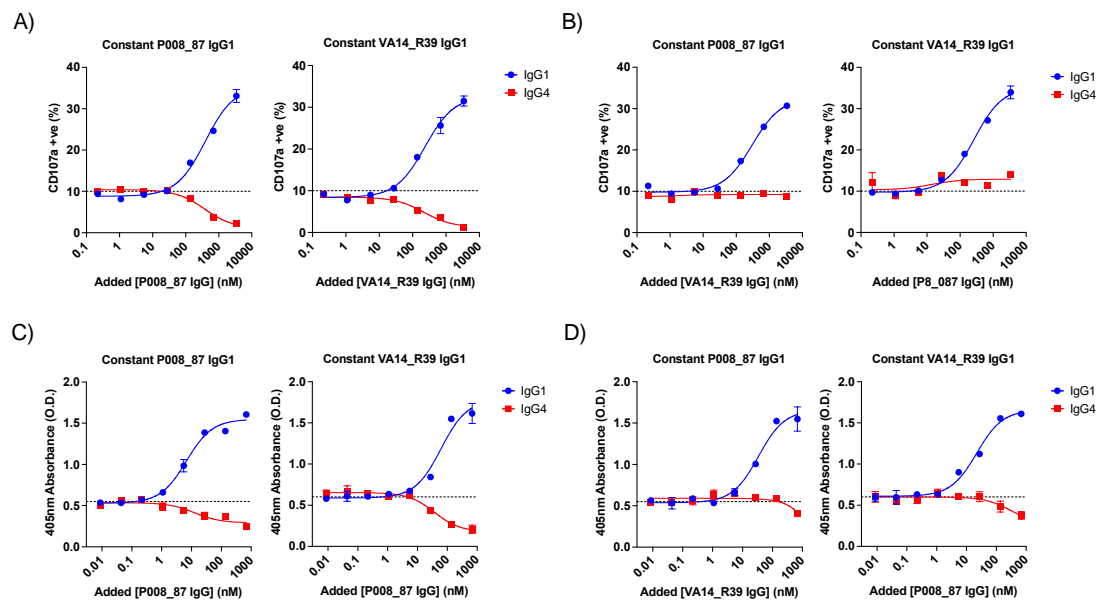
Fig. 5. Effector function competition assays between IgG1 and IgG4. (A) ADCC competition assay, with constant level of either P008_87 IgG1 or VA14_R39 IgG1 to give 10% NK cells with detectable surface CD107a, incubated with increasing amounts of the same antibody as an IgG1 (blue) or IgG4 (red). **(B)** ADCC competition assay with constant level of either P008_87 IgG1 or VA14_R39 IgG1 to give 10% of NK cells surface CD107a, incubated with increasing amounts of the other non-competitively binding antibody. **(C)** ADCD competition assay with constant level of either P008_87 IgG1 or VA14_R39 IgG1, incubated with increasing amounts of the same antibody as IgG1 (blue) or IgG4 (red). **(D)** ADCD competition assay with constant level of P008_87 IgG1 or VA14_R39 IgG1, incubated with increasing amounts of the other non-competitively binding antibody. Data representative of 2 technical replicates.

Acknowledgements:

710

711   **References:**

712   Aalberse, R.C., van der Gaag, R., and van Leeuwen, J. (1983). Serologic aspects of IgG4
713   antibodies. I. Prolonged immunization results in an IgG4-restricted response. J Immunol *130*,
714   722-726.
715   Akhtar, M., Islam, M.R., Khaton, F., Soltana, U.H., Jafrin, S.A., Rahman, S.I.A., Tauheed, I.,
716   Ahmed, T., Khan, II, Akter, A.*, et al.* (2023). Appearance of tolerance-induction and non-
717   inflammatory SARS-CoV-2 spike-specific IgG4 antibodies after COVID-19 booster
718   vaccinations. Front Immunol *14*, 1309997.
719   Aricescu, A.R., Lu, W., and Jones, E.Y. (2006). A time- and cost-efficient system for high-level
720   protein production in mammalian cells. Acta Crystallogr D Biol Crystallogr *62*, 1243-1250.
721   Baden, L.R., El Sahly, H.M., Essink, B., Kotloff, K., Frey, S., Novak, R., Diemert, D., Spector,
722   S.A., Rouphael, N., Creech, C.B.*, et al.* (2021). Efficacy and Safety of the mRNA-1273 SARS-
723   CoV-2 Vaccine. N Engl J Med *384*, 403-416.
724   Bartsch, Y.C., Cizmeci, D., Kang, J., Gao, H., Shi, W., Chandrashekar, A., Collier, A.Y., Chen,
725   B., Barouch, D.H., and Alter, G. (2023). Selective SARS-CoV2 BA.2 escape of antibody
726   Fc/Fc-receptor interactions. iScience *26*, 106582.
727   Beaudoin-Bussieres, G., and Finzi, A. (2024). Deciphering Fc-effector functions against
728   SARS-CoV-2. Trends Microbiol *32*, 756-768.
729   Bok, K., Sitar, S., Graham, B.S., and Mascola, J.R. (2021). Accelerated COVID-19 vaccine
730   development: milestones, lessons, and prospects. Immunity *54*, 1636-1651.
731   Bruhns, P., Iannascoli, B., England, P., Mancardi, D.A., Fernandez, N., Jorieux, S., and Daeron,
732   M. (2009). Specificity and affinity of human Fcgamma receptors and their polymorphic
733   variants for human IgG subclasses. Blood *113*, 3716-3725.
734   Buhre, J.S., Pongracz, T., Kunsting, I., Lixenfeld, A.S., Wang, W., Nouta, J., Lehrian, S.,
735   Schmelter, F., Lunding, H.B., Duhring, L.*, et al.* (2022). mRNA vaccines against SARS-CoV-
736   2 induce comparably low long-term IgG Fc galactosylation and sialylation levels but increasing
737   long-term IgG4 responses compared to an adenovirus-based vaccine. Front Immunol *13*,
738   1020844.
739   Cassel, D.L., Keller, M.A., Surrey, S., Schwartz, E., Schreiber, A.D., Rappaport, E.F., and
740   McKenzie, S.E. (1993). Differential expression of Fc gamma RIIA, Fc gamma RIIB and Fc
741   gamma RIIC in hematopoietic cells: analysis of transcripts. Mol Immunol *30*, 451-460.
742   Chan, C.E.Z., Seah, S.G.K., Chye, H., Massey, S., Torres, M., Lim, A.P.C., Wong, S.K.K., Neo,
743   J.J.Y., Wong, P.S., Lim, J.H.*, et al.* (2021). The Fc-mediated effector functions of a potent
744   SARS-CoV-2 neutralizing antibody, SC31, isolated from an early convalescent COVID-19

patient, are essential for the optimal therapeutic efficacy of the antibody. PLoS One *16*, e0253487.

Clark, J.J., Hoxie, I., Adelsberg, D.C., Sapse, I.A., Andreata-Santos, R., Yong, J.S., Amanat, F., Tcheou, J., Raskin, A., Singh, G*., et al.* (2024). Protective effect and molecular mechanisms of human non-neutralizing cross-reactive spike antibodies elicited by SARS-CoV-2 mRNA vaccination. Cell Rep *43*, 114922.

DiLillo, D.J., Tan, G.S., Palese, P., and Ravetch, J.V. (2014). Broadly neutralizing hemagglutinin stalk-specific antibodies require FcgammaR interactions for protection against influenza virus in vivo. Nat Med *20*, 143-151.

Fielding, C.A., Sabberwal, P., Williamson, J.C., Greenwood, E.J.D., Crozier, T.W.M., Zelek, W., Seow, J., Graham, C., Huettner, I., Edgeworth, J.D*., et al.* (2022). SARS-CoV-2 host-shutoff impacts innate NK cell functions, but antibody-dependent NK activity is strongly activated through non-spike antibodies. Elife *11*.

Fleit, H.B., and Kobasiuk, C.D. (1991). The human monocyte-like cell line THP-1 expresses Fc gamma RI and Fc gamma RII. J Leukoc Biol *49*, 556-565.

Gaebler, C., Wang, Z., Lorenzi, J.C.C., Muecksch, F., Finkin, S., Tokuyama, M., Cho, A., Jankovic, M., Schaefer-Babajew, D., Oliveira, T.Y*., et al.* (2021). Evolution of antibody immunity to SARS-CoV-2. Nature *591*, 639-644.

Gelderloos, A.T., Verheul, M.K., Middelhof, I., de Zeeuw-Brouwer, M.L., van Binnendijk, R.S., Buisman, A.M., and van Kasteren, P.B. (2024). Repeated COVID-19 mRNA vaccination results in IgG4 class switching and decreased NK cell activation by S1-specific antibodies in older adults. Immun Ageing *21*, 63.

Goldblatt, D., Alter, G., Crotty, S., and Plotkin, S.A. (2022). Correlates of protection against SARS-CoV-2 infection and COVID-19 disease. Immunol Rev *310*, 6-26.

Gorman, M.J., Patel, N., Guebre-Xabier, M., Zhu, A.L., Atyeo, C., Pullen, K.M., Loos, C., Goez-Gazi, Y., Carrion, R., Jr., Tian, J.H*., et al.* (2021). Fab and Fc contribute to maximal protection against SARS-CoV-2 following NVX-CoV2373 subunit vaccine with Matrix-M vaccination. Cell Rep Med *2*, 100405.

Graham, C., Lechmere, T., Rehman, A., Seow, J., Kurshan, A., Huettner, I., Maguire, T.J.A., Tam, J.C.H., Cox, D., Ward, C*., et al.* (2022). The effect of Omicron breakthrough infection and extended BNT162b2 booster dosing on neutralization breadth against SARS-CoV-2 variants of concern. PLoS Pathog *18*, e1010882.

Graham, C., Seow, J., Huettner, I., Khan, H., Kouphou, N., Acors, S., Winstone, H., Pickering, S., Galao, R.P., Dupont, L*., et al.* (2021). Neutralization potency of monoclonal antibodies recognizing dominant and subdominant epitopes on SARS-CoV-2 Spike is impacted by the B.1.1.7 variant. Immunity *54*, 1276-1289.

Hartley, G.E., Fryer, H.A., Gill, P.A., Boo, I., Bornheimer, S.J., Hogarth, P.M., Drummer, H.E., O'Hehir, R.E., Edwards, E.S.J., and van Zelm, M.C. (2024). Homologous but not heterologous COVID-19 vaccine booster elicits IgG4+ B-cells and enhanced Omicron subvariant binding. NPJ Vaccines *9*, 129.

Higdon, M.M., Wahl, B., Jones, C.B., Rosen, J.G., Truelove, S.A., Baidya, A., Nande, A.A., ShamaeiZadeh, P.A., Walter, K.K., Feikin, D.R*., et al.* (2022). A Systematic Review of Coronavirus Disease 2019 Vaccine Efficacy and Effectiveness Against Severe Acute Respiratory Syndrome Coronavirus 2 Infection and Disease. Open Forum Infect Dis *9*, ofac138.

Howarth, M., Liu, W., Puthenveetil, S., Zheng, Y., Marshall, L.F., Schmidt, M.M., Wittrup, K.D., Bawendi, M.G., and Ting, A.Y. (2008). Monovalent, reduced-size quantum dots for imaging receptors on living cells. Nat Methods *5*, 397-399.

Irrgang, P., Gerling, J., Kocher, K., Lapuente, D., Steininger, P., Habenicht, K., Wytopil, M., Beileke, S., Schäfer, S., Zhong, J*., et al.* (2023). Class switch toward noninflammatory, spike-

795 specific IgG4 antibodies after repeated SARS-CoV-2 mRNA vaccination. Science
796 Immunology *8*.

797 Jackson, C.B., Farzan, M., Chen, B., and Choe, H. (2022). Mechanisms of SARS-CoV-2 entry
798 into cells. Nat Rev Mol Cell Biol *23*, 3-20.

799 Kim, W., Zhou, J.Q., Horvath, S.C., Schmitz, A.J., Sturtz, A.J., Lei, T., Liu, Z., Kalaidina, E.,
800 Thapa, M., Alsoussi, W.B.*, et al.* (2022). Germinal centre-driven maturation of B cell response
801 to mRNA vaccination. Nature *604*, 141-145.

802 Kirsebom, F.C.M., Andrews, N., Stowe, J., Ramsay, M., and Lopez Bernal, J. (2023). Duration
803 of protection of ancestral-strain monovalent vaccines and effectiveness of bivalent BA.1
804 boosters against COVID-19 hospitalisation in England: a test-negative case-control study.
805 Lancet Infect Dis *23*, 1235-1243.

806 Lee, I.T., Cosgrove, C.A., Moore, P., Bethune, C., Nally, R., Bula, M., Kalra, P.A., Clark, R.,
807 Dargan, P.I., Boffito, M.*, et al.* (2023). Omicron BA.1-containing mRNA-1273 boosters
808 compared with the original COVID-19 vaccine in the UK: a randomised, observer-blind,
809 active-controlled trial. Lancet Infect Dis *23*, 1007-1019.

810 Mercado, N.B., Zahn, R., Wegmann, F., Loos, C., Chandrashekar, A., Yu, J., Liu, J., Peter, L.,
811 McMahan, K., Tostanoski, L.H.*, et al.* (2020). Single-shot Ad26 vaccine protects against
812 SARS-CoV-2 in rhesus macaques. Nature *586*, 583-588.

813 Motta, R.V., and Culver, E.L. (2024). IgG4 autoantibodies and autoantigens in the context of
814 IgG4-autoimmune disease and IgG4-related disease. Front Immunol *15*, 1272084.

815 Mozdzanowska, K., Feng, J., and Gerhard, W. (2003). Virus-neutralizing activity mediated by
816 the Fab fragment of a hemagglutinin-specific antibody is sufficient for the resolution of
817 influenza virus infection in SCID mice. J Virol *77*, 8322-8328.

818 Muecksch, F., Wang, Z., Cho, A., Gaebler, C., Ben Tanfous, T., DaSilva, J., Bednarski, E.,
819 Ramos, V., Zong, S., Johnson, B.*, et al.* (2022). Increased Memory B Cell Potency and Breadth
820 After a SARS-CoV-2 mRNA Boost. Nature.

821 Olivieri, D.N., and Gambon Deza, F. (2018). Immunoglobulin genes in Primates. Mol Immunol
822 *101*, 353-363.

823 Parhiz, H., Atochina-Vasserman, E.N., and Weissman, D. (2024). mRNA-based therapeutics:
824 looking beyond COVID-19 vaccines. Lancet *403*, 1192-1204.

825 Pierre, C.N., Adams, L.E., Higgins, J.S., Anasti, K., Goodman, D., Mielke, D., Stanfield-
826 Oakley, S., Powers, J.M., Li, D., Rountree, W.*, et al.* (2024). Non-neutralizing SARS-CoV-2
827 N-terminal domain antibodies protect mice against severe disease using Fc-mediated effector
828 functions. PLoS Pathog *20*, e1011569.

829 Pillai, S. (2023). Is it bad, is it good, or is IgG4 just misunderstood? Sci Immunol *8*, eadg7327.

830 Polack, F.P., Thomas, S.J., Kitchin, N., Absalon, J., Gurtman, A., Lockhart, S., Perez, J.L.,
831 Perez Marc, G., Moreira, E.D., Zerbini, C.*, et al.* (2020). Safety and Efficacy of the BNT162b2
832 mRNA Covid-19 Vaccine. N Engl J Med *383*, 2603-2615.

833 Polycarpou, A.e.a. (2023). The complement pattern recognition molecule CL-11 promotes
834 invasion and injury of respiratory epithelial cells by SARS-CoV-2. bioRxiv.

835 Qin, L., Tang, L.F., Cheng, L., and Wang, H.Y. (2022). The clinical significance of allergen-
836 specific IgG4 in allergic diseases. Front Immunol *13*, 1032909.

837 Rispens, T., and Huijbers, M.G. (2023). The unique properties of IgG4 and its roles in health
838 and disease. Nat Rev Immunol *23*, 763-778.

839 Roltgen, K., Nielsen, S.C.A., Silva, O., Younes, S.F., Zaslavsky, M., Costales, C., Yang, F.,
840 Wirz, O.F., Solis, D., Hoh, R.A.*, et al.* (2022). Immune imprinting, breadth of variant
841 recognition, and germinal center response in human SARS-CoV-2 infection and vaccination.
842 Cell *185*, 1025-1040 e1014.

843 Rosa, A., Pye, V.E., Graham, C., Muir, L., Seow, J., Ng, K.W., Cook, N.J., Rees-Spear, C.,
844 Parker, E., Silva Dos Santos, M., *et al.* (2021). SARS-CoV-2 can recruit a haem metabolite to
845 evade antibody immunity. Sci Adv *7*, eabg7607.

846 Santos, A.F., James, L.K., Bahnson, H.T., Shamji, M.H., Couto-Francisco, N.C., Islam, S.,
847 Houghton, S., Clark, A.T., Stephens, A., Turcanu, V., *et al.* (2015). IgG4 inhibits peanut-
848 induced basophil and mast cell activation in peanut-tolerant children sensitized to peanut major
849 allergens. J Allergy Clin Immunol *135*, 1249-1256.

850 Schafer, A., Muecksch, F., Lorenzi, J.C.C., Leist, S.R., Cipolla, M., Bournazos, S., Schmidt,
851 F., Maison, R.M., Gazumyan, A., Martinez, D.R., *et al.* (2021). Antibody potency, effector
852 function, and combinations in protection and therapy for SARS-CoV-2 infection in vivo. J Exp
853 Med *218*.

854 Seow, J., Graham, C., Hallett, S.R., Lechmere, T., Maguire, T.J.A., Huettner, I., Cox, D., Khan,
855 H., Pickering, S., Roberts, R., *et al.* (2022). ChAdOx1 nCoV-19 vaccine elicits monoclonal
856 antibodies with cross-neutralizing activity against SARS-CoV-2 viral variants. Cell Rep,
857 110757.

858 Seow, J., Graham, C., Merrick, B., Acors, S., Pickering, S., Steel, K.J.A., Hemmings, O.,
859 O'Byrne, A., Kouphou, N., Galao, R.P., *et al.* (2020). Longitudinal observation and decline of
860 neutralizing antibody responses in the three months following SARS-CoV-2 infection in
861 humans. Nat Microbiol *5*, 1598-1607.

862 Sokal, A., Chappert, P., Barba-Spaeth, G., Roeser, A., Fourati, S., Azzaoui, I., Vandenberghe,
863 A., Fernandez, I., Meola, A., Bouvier-Alias, M., *et al.* (2021). Maturation and persistence of
864 the anti-SARS-CoV-2 memory B cell response. Cell *184*, 1201-1213 e1214.

865 Tiller, T., Meffre, E., Yurasov, S., Tsuiji, M., Nussenzweig, M.C., and Wardemann, H. (2008).
866 Efficient generation of monoclonal antibodies from single human B cells by single cell RT-
867 PCR and expression vector cloning. J Immunol Methods *329*, 112-124.

868 Tostanoski, L.H., Wegmann, F., Martinot, A.J., Loos, C., McMahan, K., Mercado, N.B., Yu, J.,
869 Chan, C.N., Bondoc, S., Starke, C.E., *et al.* (2020). Ad26 vaccine protects against SARS-CoV-
870 2 severe clinical disease in hamsters. Nat Med *26*, 1694-1700.

871 Turner, J.S., O'Halloran, J.A., Kalaidina, E., Kim, W., Schmitz, A.J., Zhou, J.Q., Lei, T., Thapa,
872 M., Chen, R.E., Case, J.B., *et al.* (2021). SARS-CoV-2 mRNA vaccines induce persistent
873 human germinal centre responses. Nature *596*, 109-113.

874 UKHSA (2022). SARS-CoV-2 variants of concern and variants under investigation in England,
875 number 34.

876 Unger, P.P., Makuch, M., Aalbers, M., Derksen, N.I.L., Ten Brinke, A., Aalberse, R.C., Rispens,
877 T., and van Ham, S.M. (2018). Repeated vaccination with tetanus toxoid of plasma donors with
878 pre-existing specific IgE transiently elevates tetanus-specific IgE but does not induce allergic
879 symptoms. Clin Exp Allergy *48*, 479-482.

880 Urban, M., Winkler, T., Landini, M.P., Britt, W., and Mach, M. (1994). Epitope-specific
881 distribution of IgG subclasses against antigenic domains on glycoproteins of human
882 cytomegalovirus. J Infect Dis *169*, 83-90.

883 van de Veen, W., Globinska, A., Jansen, K., Straumann, A., Kubo, T., Verschoor, D., Wirz, O.F.,
884 Castro-Giner, F., Tan, G., Ruckert, B., *et al.* (2020). A novel proangiogenic B cell subset is
885 increased in cancer and chronic inflammation. Sci Adv *6*, eaaz3559.

886 Van den Hoecke, S., Ehrhardt, K., Kolpe, A., El Bakkouri, K., Deng, L., Grootaert, H.,
887 Schoonooghe, S., Smet, A., Bentahir, M., Roose, K., *et al.* (2017). Hierarchical and Redundant
888 Roles of Activating FcgammaRs in Protection against Influenza Disease by M2e-Specific IgG1
889 and IgG2a Antibodies. J Virol *91*.

890 van der Neut Kolfschoten, M., Schuurman, J., Losen, M., Bleeker, W.K., Martinez-Martinez,
891 P., Vermeulen, E., den Bleker, T.H., Wiegman, L., Vink, T., Aarden, L.A., *et al.* (2007). Anti-

892   inflammatory activity of human IgG4 antibodies by dynamic Fab arm exchange. Science *317*,
893   1554-1557.

894   Vidarsson, G., Dekkers, G., and Rispens, T. (2014). IgG subclasses and allotypes: from
895   structure to effector functions. Frontiers in Immunology *5*.

896   Walls, A.C., Park, Y.J., Tortorici, M.A., Wall, A., McGuire, A.T., and Veesler, D. (2020).
897   Structure, Function, and Antigenicity of the SARS-CoV-2 Spike Glycoprotein. Cell *183*, 1735.

898   Wilson, C., Ebling, R., Henig, C., Adler, T., Nicolaevski, R., Barak, M., Cazabon, J., Maisin,
899   D., Lepoutre, T., Gruson, D.*, et al.* (2013). Significant, quantifiable differences exist between
900   IgG subclass standards WHO67/97 and ERM-DA470k and can result in different interpretation
901   of results. Clin Biochem *46*, 1751-1755.

902   Winkler, E.S., Gilchuk, P., Yu, J., Bailey, A.L., Chen, R.E., Chong, Z., Zost, S.J., Jang, H.,
903   Huang, Y., Allen, J.D.*, et al.* (2021). Human neutralizing antibodies against SARS-CoV-2
904   require intact Fc effector functions for optimal therapeutic protection. Cell *184*, 1804-1820
905   e1816.

906   Wratil, P.R., Stern, M., Priller, A., Willmann, A., Almanzar, G., Vogel, E., Feuerherd, M.,
907   Cheng, C.C., Yazici, S., Christa, C.*, et al.* (2022). Three exposures to the spike protein of
908   SARS-CoV-2 by either infection or vaccination elicit superior neutralizing immunity to all
909   variants of concern. Nat Med *28*, 496-503.

910   Yamin, R., Jones, A.T., Hoffmann, H.H., Schafer, A., Kao, K.S., Francis, R.L., Sheahan, T.P.,
911   Baric, R.S., Rice, C.M., Ravetch, J.V.*, et al.* (2021). Fc-engineered antibody therapeutics with
912   improved anti-SARS-CoV-2 efficacy. Nature *599*, 465-470.

913   Zelek, W.M., Harris, C.L., and Morgan, B.P. (2018). Extracting the barbs from complement
914   assays: Identification and optimisation of a safe substitute for traditional buffers.
915   Immunobiology *223*, 744-749.

916   Zhang, A., Stacey, H.D., D'Agostino, M.R., Tugg, Y., Marzok, A., and Miller, M.S. (2023).
917   Beyond neutralization: Fc-dependent antibody effector functions in SARS-CoV-2 infection.
918   Nat Rev Immunol *23*, 381-396.

919   Zohar, T., Atyeo, C., Wolf, C.R., Logue, J.K., Shuey, K., Franko, N., Choi, R.Y., Wald, A.,
920   Koelle, D.M., Chu, H.Y.*, et al.* (2022). A multifaceted high-throughput assay for probing
921   antigen-specific antibody-mediated primary monocyte phagocytosis and downstream
922   functions. J Immunol Methods *510*, 113328.

923   Zufferey, R., Nagy, D., Mandel, R.J., Naldini, L., and Trono, D. (1997). Multiply attenuated
924   lentiviral vector achieves efficient gene delivery in vivo. Nat Biotechnol *15*, 871-875.

925

926